



Brazilian Journal of Physics

ISSN: 0103-9733

luizno.bjp@gmail.com

Sociedade Brasileira de Física

Brasil

Vivanco, F. J.; de Paiva, R. R.; Pedrozo-Peñafiel, E.; Farias, K. M.; Bagnato, V. S.  
A Simplified Method for Identification of the Vibrational Series of Long-Range States in

Na<sub>2</sub>

Brazilian Journal of Physics, vol. 45, núm. 3, junio, 2015, pp. 272-279

Sociedade Brasileira de Física

São Paulo, Brasil

Available in: <http://www.redalyc.org/articulo.oa?id=46439436002>

- How to cite
- Complete issue
- More information about this article
- Journal's homepage in redalyc.org

redalyc.org

Scientific Information System

Network of Scientific Journals from Latin America, the Caribbean, Spain and Portugal

Non-profit academic project, developed under the open access initiative

# A Simplified Method for Identification of the Vibrational Series of Long-Range States in Na<sub>2</sub>

F. J. Vivanco · R. R. de Paiva · E. Pedrozo-Peñafiel ·  
K. M. Farias · V. S. Bagnato

Received: 9 January 2015 / Published online: 8 April 2015  
© Sociedade Brasileira de Física 2015

**Abstract** We performed two-color photoassociative ionization experiments in cold sodium atoms in a dark MOT. We produce a sample where most of the atoms were in the ground hyperfine state  $F = 1$ . Applying a laser with variable frequency, in the region of 0 to  $-32$  GHz, we obtained a photoassociative spectra containing sequences of different long-range potentials. Using the scaling law for intermediate states, we identified the vibrational series of involved states, separating the sequences. In this way, we have identified the vibrational series for the  $1_g$ ,  $0_u^+$ , and  $0_g^-$  states contributions.

**Keywords** Photoassociative ionization · Magneto-optical trap · Sodium atoms · Long-range potential

## 1 Introduction

In the field of atomic interactions, long-range states are dominant when describing cold collisions in trapped atoms. When two atoms approach each other, they interact and experience a force that can be described by an interatomic potential. This interaction is dominated by different effects depending on the distance between the nuclei of the atoms. If they are far apart, the radial wave functions do not overlap, and thus, the interaction is caused almost exclusively by the Coulomb force that is a long-range force. As they approach each other, the interaction becomes dominated by the overlapping of their radial wave functions.

For Na-Na collision, the long-range states have been extensively studied in the past years [1]. The interest of this work is only in those attractive potentials that admit bound states connected asymptotically with the dissociation limit  $3^2S_{1/2} + 3^2P_{1/2}$  (see Fig. 1). Thus, the only potentials that can contribute are the  $0_u^+$ ,  $0_g^-$ ,  $1_g$ ,  $1_u$ , and  $2_u$  states. Due to selection rules, we exclude the  $2_u$  state since we cannot excite from a ground state  $\Sigma'$  to the  $2_u$  state [2]. Other state that does not appear in the photoassociative ionization spectrum is the  $1_u$  state because the detuning from transition to excite this state is approximately 5 MHz, while the typical detuning used in the experiments is larger than that [3].

The low-energy internal structure of a diatomic molecule, like the Na<sub>2</sub> molecule, makes possible the development and advances in several areas as atomic physics and chemistry, applications in quantum simulation [4], precision measurement [5], cold chemistry [6], and quantum information [7].

## 2 Scaling Law for Intermediate States

Stwalley [10] calculated the sequence of long-range states using a simple method. Briefly, it is the improvement of the one proposed by Movre and Prichler [9], where the energies of vibrational levels close to the dissociation limit in the single-excited potential can be approximated by  $C_3/R^3$ , and it obeys the semi-classical relation:

$$v - v_D = a_3 \epsilon_v^{1/6}, \quad (1)$$

with

$$a_3 = \frac{2(2\mu\pi)^{1/2}}{h} \frac{\Gamma(5/6)}{\Gamma(4/3)} C_3^{1/3}, \quad (2)$$

F. J. Vivanco (✉) · R. R. de Paiva · E. Pedrozo-Peñafiel ·  
K. M. Farias · V. S. Bagnato  
Instituto de Física de São Carlos, Universidade de São Paulo,  
CP 369, 13560-970 São Carlos, São Paulo, Brasil  
e-mail: franklinze@gmail.com

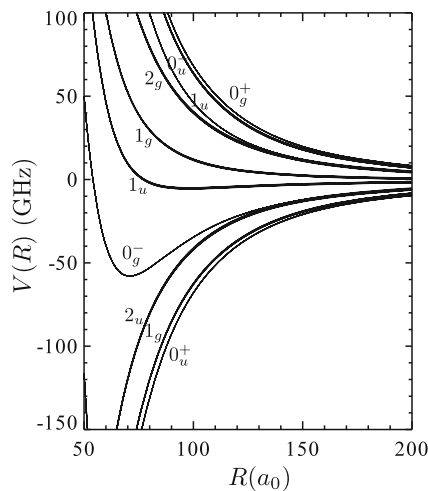


**Fig. 1** The intermediate states for the  $\text{Na}_2$  molecule connected with  $3^2S_{1/2} + 3^2P_{1/2}$ . Adapted from [8]

and  $\epsilon_v = E_D - E_{v=0}$ .  $v_D$  is the vibrational number for the vibrational level for the dissociation limit, and  $v$  is the effective vibrational quantum number of interest.  $\Gamma(5/6)$  and  $\Gamma(4/3)$  are gamma numbers,  $\mu$  is the reduced mass of two atoms, and  $h$  the Planck's constant. The coefficient  $a_3$  is calculated from perturbation theory. The relationship given by (1) makes possible the identification of the vibrational levels, which is the main purpose of this report.

### 3 Experimental System

In a magneto-optical trap (MOT) for sodium atoms, one laser beam with tunable wavelength is added. The laser frequency could be detuned from the atomic transition (508.84801 GHz) up to 32 GHz, to the red or the blue side. The experimental system for MOT [16] consist of an oven at 550 K from which atoms are ejected and subsequently decelerated by a Zeeman slower to the chamber which has a pressure of the order of  $10^{-9}$  Torr. This system allows us to trap about  $5 \times 10^9$  atoms. The slowing and trapping of sodium atoms involve the use of various laser frequencies, which were obtained from a solid state laser SHG Toptica®, by using acousto-optical modulators (AOM) and electro-optical modulators (EOM). Figure 2 shows the energy levels of interest for a sodium MOT.

For a cooling process, a cyclic transition is required. The sodium atoms excited by the cooling beam return to the ground state and scattered a photon. For sodium atoms, the D2 line transition  $F = 2 \rightarrow F' = 3$  have a large dipole moment and therefore is more suitable for cooling the atoms. Also, we have an additional effect to be considered: the atoms can make an undesired transition from the  $F' = 2$  state to  $F = 1$  state. To recover these atoms in the cooling

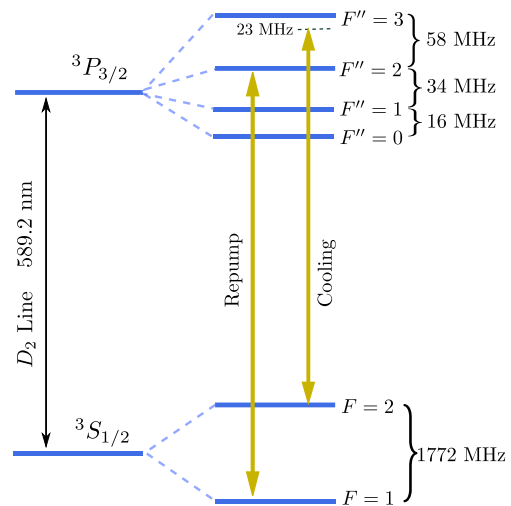


**Fig. 2** Structure of hyperfine levels in sodium atom. The corresponding frequencies to the cooling and repump are shown

process, a repump beam, tuned close to this transition, is used. Thus, the sodium atoms can reach very low temperatures to be trapped. The experimental system for producing our MOT is shown schematically in Fig. 3.

The necessity to obtain high densities in samples of cold atoms began to be evident when this samples were used as a step towards the Bose-Einstein condensation [11]. In a current MOT (called Bright MOT), the atoms are mostly (99 %) in the hyperfine state  $F = 2$ . In this configuration, the density is limited due to the collision process among the atoms, in which part of the excitation energy is converted into kinetic energy, which causes atoms to escape from the MOT. As an alternative to this problem, the so-called dark spot MOT or dark MOT was proposed and developed by Ketterle at MIT [12]. In a dark MOT, one spot is positioned in the middle of repump beam, with the result that the central volume of the trap is free of repump light. Thus, most of the trapped atoms (about 99 %) are optically pumped predominant to the fundamental hyperfine level  $F = 1$  where they do not interact with the trapping light. Thus, there are atoms in  $F = 1$ . As a direct result of this, the density of the atoms in the dark MOT is larger than that in a current bright MOT.

Experimentally, the addition of the dark spot in the repump beam is not sufficient to obtain a robust dark MOT. This is because there are edge effects that lead to having a repump beam entering the chamber with the center not dark enough. To overcome this problem, the dark spot beam is focused and we put a iris in the focus to avoid the edge effects; an extra lens is used to collimate this beam to the experiment (see the Fig. 3). With this method, we get a dark spot totally dark in the center with a MOT density of approximately  $5 \times 10^{11}$  atoms/cm<sup>3</sup>.

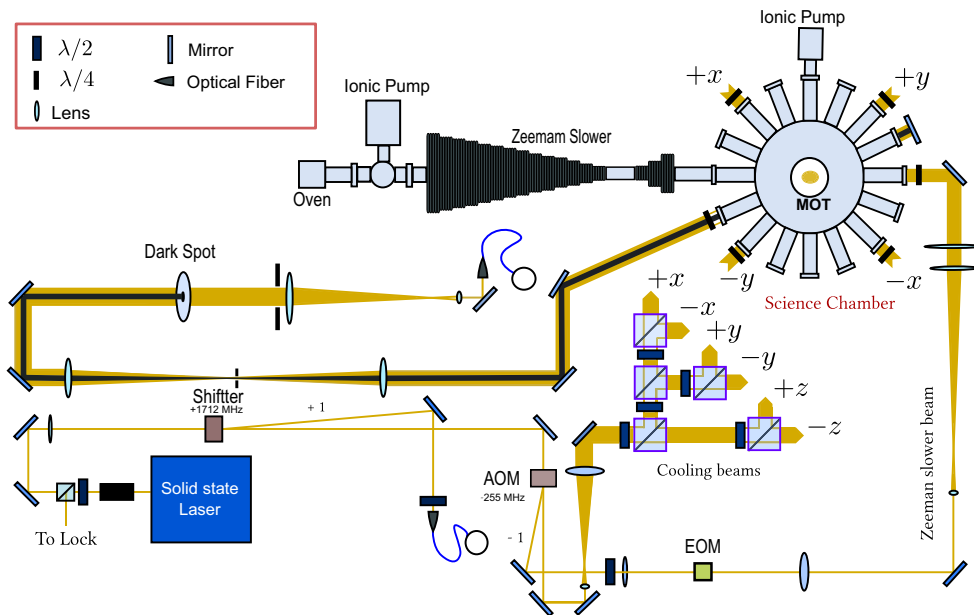


**Fig. 3** Experimental setup for the dark MOT production. AOMs are used for producing the necessary frequencies for cooling, repump, and slower (with additional EOM)

### 3.1 Photoassociative Ionization

In cold sodium atoms, PAI spectra are common tools to detect and identify the processes in collision experiments at low energies. Since it was first proposed as a spectroscopy technique in 1989 by Thorsheim [13, 14], it has been

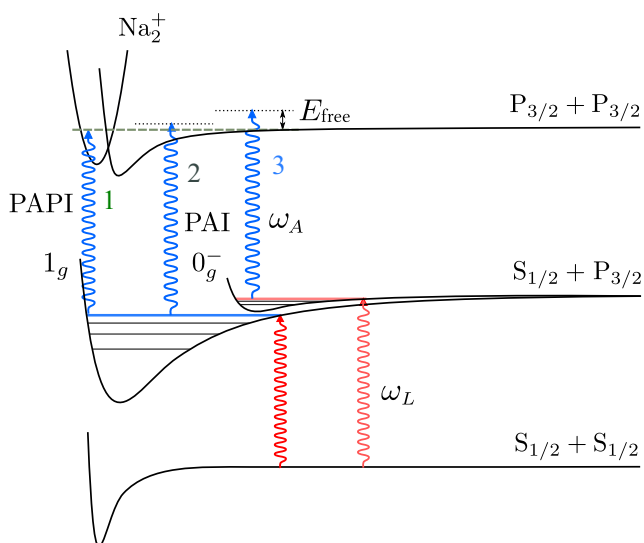


**Fig. 4** Diagram for two-color PAI for  $\text{Na}_2$ . The path of photoionization depends on the energies of the photons involved in the process. 1 Photoionization to small distances, directly in the continuum state, know like photoassociative photoionization (PAPI). 2 Process that involved the  $1_g$  state and after a double excited state. 3 Process that involve a purely long-range state ( $0_g^-$ ) and after a double excited state. The last process is of the most probability in the experiments when two-color PAI are performed

improved to be a common practice in laboratories which study cold atoms. The PAI is a process in which a colliding atomic pair in the fundamental molecular state absorbs a photon and passes to a first excited molecular state. A second step is required in order to ionize one of the atoms so it can be detected. The product of this reaction is one or more electrons which may be detected with a ion counter or in a decrease of the atomic fluorescence of the sample. The PAI may involve only photons with a single frequency, making both the process of excitation and ionization (commonly with a detuning to the red of the atomic transition) or may involve photons with two frequencies, one doing the excitation to the first molecular state (with detuning for the red transition) and another doing the step of ionizing (blue detuning of the atomic transition). The first case is called single-color PAI, and the second one is the two-color PAI [15]. Figure 4 shows this process for sodium atoms.

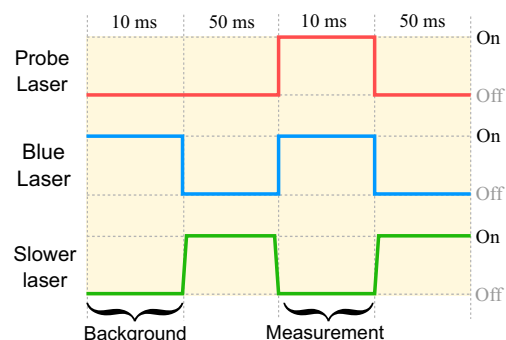


**Fig. 5** Scheme of the temporal sequence implemented in this experiment and controlled by Labview®

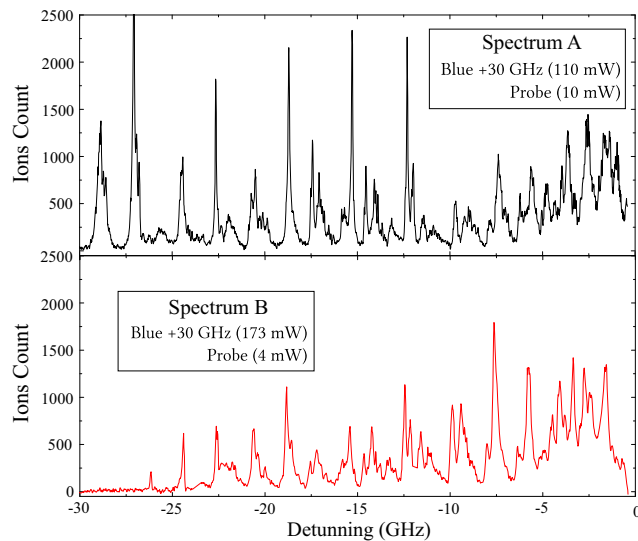


**Fig. 6** Two-color PAI spectra for sodium atoms in the region of 0 to  $-32$  GHz

#### 4 Experimental Results and Discussion

We performed two-color photoassociative ionization (PAI) in Na atoms trapped in a dark MOT, using two laser beams obtained from dye lasers Coherent® 899 and Coherent® 699. These laser beams are focused on the sample with an effective incidence area of  $3.4 \times 10^{-2} \text{ mm}^2$ . Both lasers go through the same window of the main chamber with intensity profiles on the same order. For a better resolution in the PAI spectrum, a temporal sequence was implemented, which is shown in Fig. 5. This temporal sequence was performed by mechanical shutters and basically consists of four steps: (1) turn off the slower beam and turn on the blue beam for 10 ms. The background ion count is performed in this interval; (2) turn off the blue beam and turn on the

slower beam for 50 ms in order to retrieve the sample of cold atoms; (3) turn off the slower beam again and turn on the blue and probe beams for the same time interval from step 1 and make another ion count, which we named Measurement; and (4) turn off the blue and probe beams and turn on the slower beam for the same interval of the step 2, leaving the system ready to begin a new measure. The effective ion count is given by subtracting the Background from the measurement.

The entire system of the temporal sequence and the operation system of the laser is controlled and monitored by commercial interface from National Instruments®, associated to a homemade program based in Labview®. As the probe laser is swept from the resonance frequency until it reaches  $-32$  GHz of detuning, it is necessary to uniformly change the intervals of measurement. For counting ions, we used an ion counter. We used a photo-detector to monitor the fluorescence of the atoms, indirectly measuring the number of trapped atoms, like we did in our past work [16].

##### 4.1 Spectrum in the Region of 0 to $-32$ GHz

It has been seen in previous works [17, 18] that the dominant states in a PAI spectrum are  $0_g^-$  and  $1_g$ . In many single- and two-color PAI experiments, the vibrational series are identified as being the series of  $0_g^-$  and  $1_g$  states, but it is known that they are not the only ones present. On a broader spectrum, as the one we obtained, we can make a more complete identification and study vibrational series of states that do not appear in spectra in which PAI has performed in a conventional MOT. The advantage of the dark MOT, is precisely that it allows the appearance of states that are absent when both colliding atoms are in the hyperfine ground state  $F = 2$ . Thus, the resulting structure now have peaks of states belonging to this type of unconventional

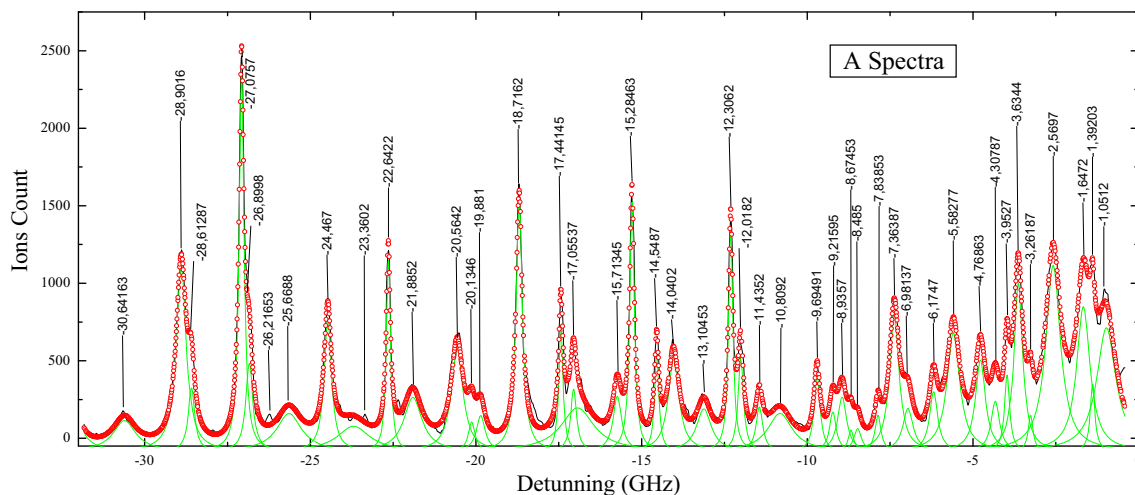


**Fig. 7** Lorentz fittings for “A” spectrum. The fitting reproduce almost all structures present in the original figure, except a peak localized in  $-26, 216$  GHz. The solid lines corresponding to individual peaks

spectrum. These new structures become interesting because they show dependence on the system configuration; we can have access to different molecular levels. This is why an identification of these structures through a scaling law will be of importance to know what type of molecular states are dealing.

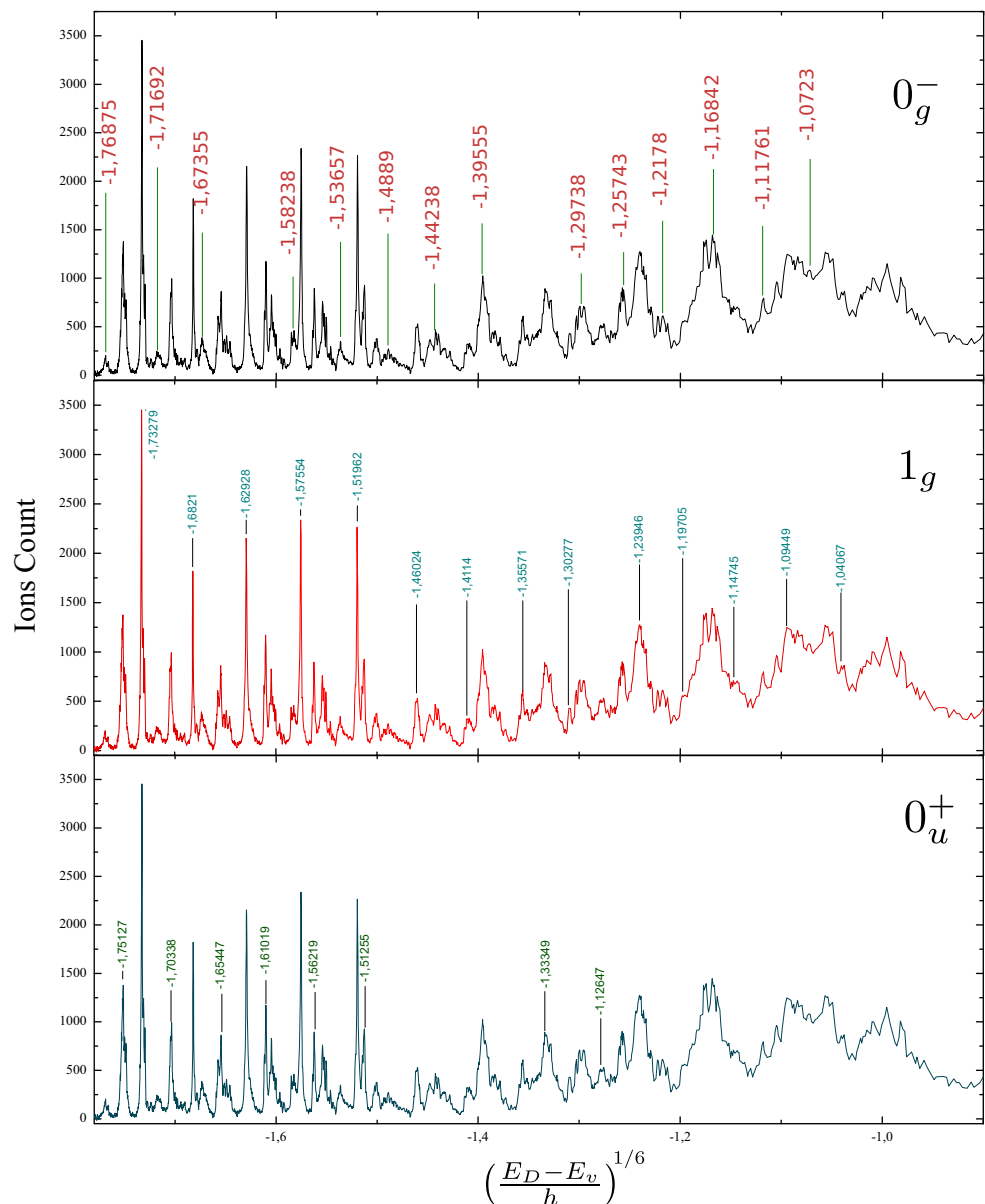
Figure 6 shows two spectra obtained for two-color PAI in a dark MOT. We call these of “A” and “B” spectra, respectively. The “A” spectrum was obtained by scanning the probe laser from 0 to  $-32$  GHz with a power of  $10$  mW ( $\sim 0,3$  W/mm<sup>2</sup>) and a blue laser with a detuning of the resonance frequency of  $+30$  GHz and a power of  $110$  mW ( $\sim 3,2$  W/mm<sup>2</sup>). In the case of “B” spectrum, we used the probe laser with a power of  $4$  mW ( $\sim 0,1$  W/mm<sup>2</sup>) with the same sweep that for the “A” spectrum and a blue laser with

a power of  $173$  mW ( $\sim 5$  W/mm<sup>2</sup>) and the detuning is also  $+30$  GHz.

In order to identify the structures present in our two-color PAI spectrum, we implemented a Lorentzian fitting on “A” and “B” spectra. The fitting made for “A” spectrum can be seen in Fig. 7. For the “B” spectrum, we have a similar adjustment. We labeled the frequencies at which most prominent resonances occur for later identification of the vibrational series using the method proposed by Stwalley [10].

In a two-color PAI experiment, the influence of the second step (in which the blue laser frequency  $\omega_A$  ionizes the atomic pair) in the spectrum can be seen reflected in the relative heights of the peaks of the states, and this effect was most evident in the pure state long-range  $0_g^-$ . This

**Fig. 8** Spectrum of the energies of the peaks of “A” to  $1/6$  exponent. The regularly spaced peaks correspond to a specific vibrational series identified. We have labeled the values of the detuning to the  $1/6$  exponent to be able to demonstrate the scaling law



highlights the importance of the second step in the PAI spectrum. Amelink shows that the peak height of the state  $0_g^-$  is related to the second step due to the structures of doubly excited state since the state  $0_g^-$  which usually only makes possible PAI in large interatomic distances [17]. He demonstrated that the doubly excited states  $1_u$  and  $0_u^-$  are the dominant routes in the PAI process for sodium atoms [20]. Here, it is assumed that the dipole moments for transitions from the ground state to the single-excited state  $0_g^-$  are independent of the vibrational quantum number and the dipole moments for transitions from any vibrational level of the single-excited state  $0_g^-$  to doubly excited states  $1_u$  and  $0_u^-$  depend on the symmetry of this doubly excited states but not on the energy excess. Thus, we must take into account that the structures corresponding to the  $0_g^-$  state will depend on the second step which is performed by the blue laser.

Many studies have made similar identifications of the vibrational series present in PAI spectra and were inspired by the original work of Stwalley. Lett [19] made a similar identification in the first 100 GHz of single-color PAI spectrum and identified the vibrational series, as being

those from  $0_g^-$  and  $1_g$  states effectively. Bagnato [1] also made a similar identification for a two-color PAI spectrum of sodium atoms in the first 3 GHz. Again, Amelink [20], using the same method with the scaling law for the corresponding doubly excited states, identified the rovibrational series for PAI spectrum of doubly excited states in the  $\text{Na}_2$  molecule. The major difference of our work is to use a dark MOT.

To make the identification of peaks, we plot our spectra (we show only the results for “A” spectrum; for the “B” spectrum we have similar results) as dependent of detuning to 1/6 power as the scaling law for intermediate molecular states. With this, we have new spectrum that will allow a better identification of vibrational series present. With the aid of a computer program, it could identify the existing three series in the whole spectrum for both “A” and “B” spectra. Figure 8 shows the spectrum raised to 1/6 for the “A” spectrum. A similar result occurs when we do the same with the “B” spectrum.

For better identification, we have taken the “A” spectrum and its reproduction by a Lorentzian fitting. Taking the

**Fig. 9** Vibrational spectrum for each series reproduced by a Lorentzian fit. Spectrum for the  $0 - g$  state, the spectrum for the  $1_g$  state, and spectrum with the structures of the  $0_u^+$  state are shown. For each of these states we have also included an inset that verifies the scaling law. The arrows indicate where there is a missing peak in the series

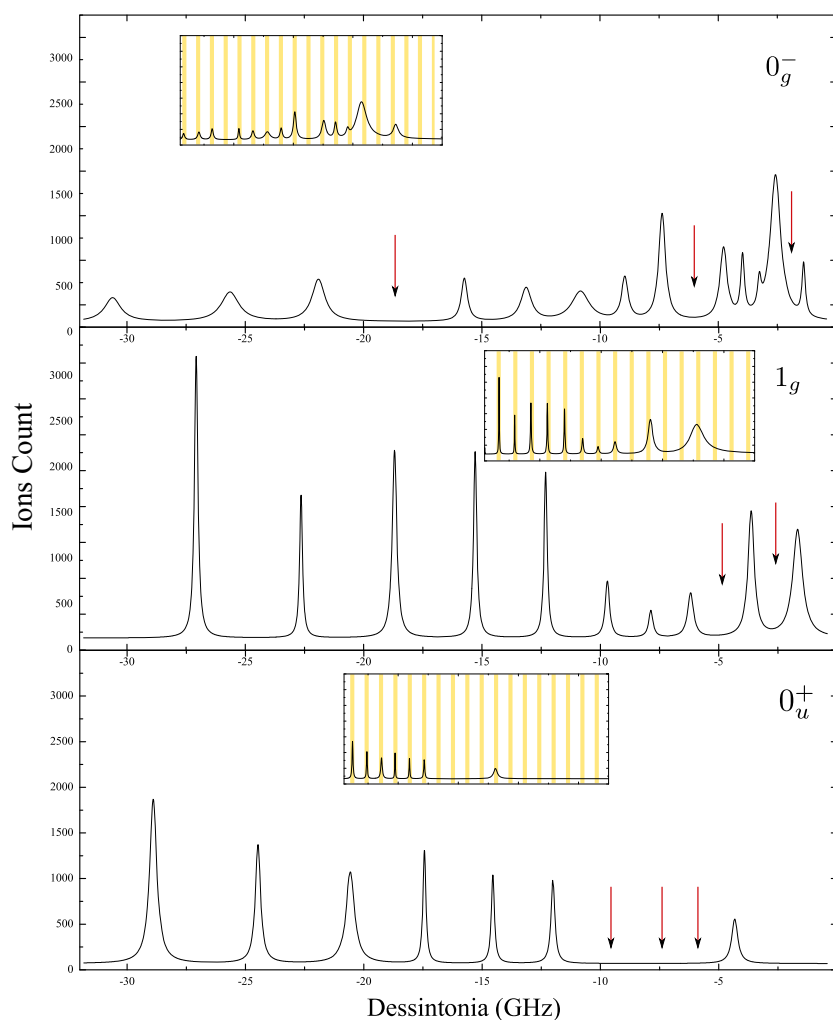
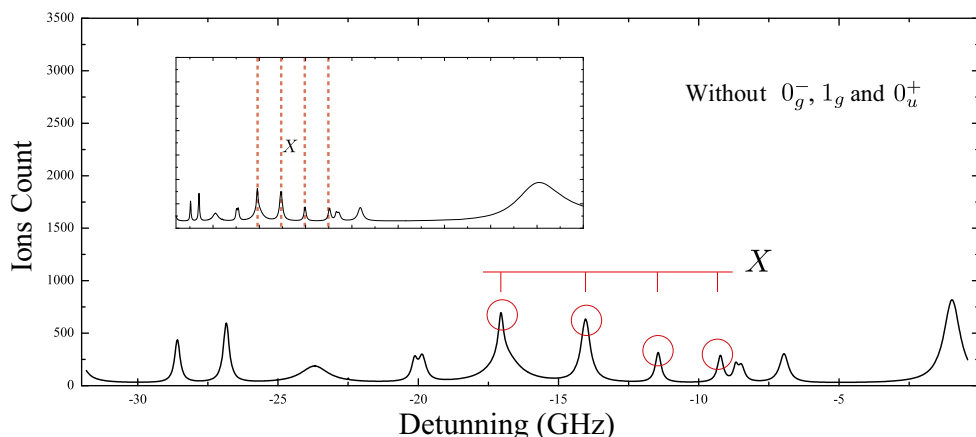




**Fig. 10** Gradually subtract each set to identify vibrational peaks in the spectrum residual. One can see that the peaks marked with circles obey a scaling law for intermediate states, which we call *X*. An inset shows the scaling law is fulfilled for the series *X*



values corresponding to frequencies where peaks occur for a particular series and put this to 6 power, retrieving the position of the peaks in original frequency can identify each peak in Fig. 7. Now taking each peak by a Lorentzian fit, we can reproduce each vibrational series in an isolated spectrum. This can be seen in Fig. 9, which have isolated the series for  $0_g^-$ ,  $1_g$  states and the other state present identified as  $0_u^+$  state. In order to identify residual peaks in our spectrum, we subtract each series of the original spectrum to see if it is just a series to be identified.

In Fig. 10, viewable spectrum with peaks remain when we subtract the series identified. The peaks highlighted by a circle are peaks that also obey a  $1/6$  scaling law.

With the values for peak vibrational series of the “A” and “B” spectra, it make a plot which determines how the vibrational series are equally spaced in a spectrum with detuning raised to the  $1/6$ . It can be seen Fig. 11 that the scaling law is obeyed in both spectra (“A” and “B”) and, moreover, are coincident vibrational for each series. Here, we have taken into account the values of the numbers for the vibrational state  $1_g$ . We have started the numbers arbitrarily since we intend here to check the scaling law and the identification

number of vibrational rather than the numbers  $v$  for each state.

We must consider other effects which were not taken into account in the identification of this spectrum, as the changes induced by the presence of the hyperfine structure, collisions of atoms corresponding to the hyperfine state  $F = 2$ , and processes induced by experimental limitations. It is important to mention that in the PAI process, the ideal was to have the MOT without interacting with external fields. Our experiment was carried out with all of these fields present in the MOT. However, we can say that the effects produced by them were minimal.

But, an interesting question arises. Which peaks correspond to the series that also obey the scaling law for simply excited molecular states and are not recognized to belong to any of the known states? Without a more resolved PAI spectra, it is difficult to answer this question. However, we can venture to say that they can be present due to a deformation in the potential presence of an intense light field, like the one we used in this experiment. A more accurate interpretation for them is beyond the scope of this work and shall be investigated in a future.

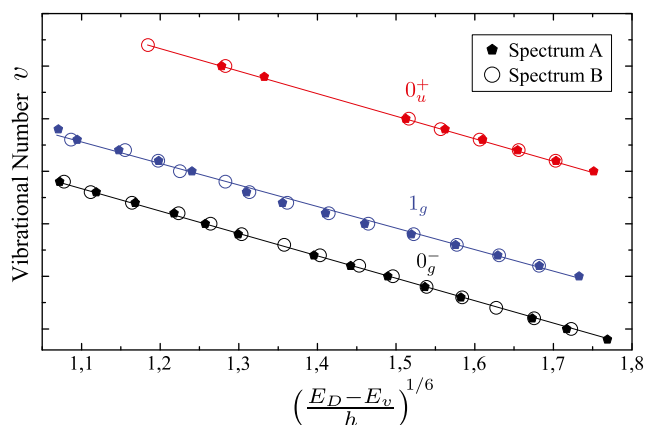


**Fig. 11** Vibrational series follow the scaling law for molecular intermediate states for both “A” and “B” spectra

## 5 Conclusion

We have measured and identified vibrational levels of a single-excited  $0_g^-$ ,  $0_u^+$ , and  $1_g$  potentials near the  $3^2S_{1/2} + 3^2P_{3/2}$  asymptote. Based on the simple method proposed for Stwalley, we identified these levels and we found four peaks obeying the scaling law but that are not part of the previews identified series. With our method, we demonstrated that it is possible to identify the vibrational series for any spectra for intermediate molecular states.

**Acknowledgments** The authors thank Reginaldo Napolitano, Marcelo Martinelli, and André Oliveira, for fruitful discussions and suggestions, to Jhonas O. Sarro and Alexandre R. Silva for the aim in the measurements, and the financial support for FAPESP (CEPID), CNPq (INCT), and CAPES.



## References

1. V.S. Bagnato, J. Weiner, P.S. Julienne, C.J. Williams, *Laser Phys.* **4**, 5 (1994)
2. W. Demtroder, *Atoms, molecules and photons* (Springer, Heidelberg, 2003)
3. A. Amelink, *Photoassociation of ultracold sodium atoms*. PhD these, Utrecht (2001)
4. I. Bloch, J. Dalibard, S. Nascimbene, *Nat. Phys.* **8**, 4 (2012)
5. F.-X. Esnault, D. Holleville, N. Rossetto, S. Guerandel, N. Dimarcq, *Phys. Rev. A* **82**, 033436 (2010)
6. S. Ospelkaus, K.-K. Ni, D. Wang, M.H.G. de Miranda, B. Neyenhuis, G. Quémener, P.S. Julienne, J.L. Bohn, D.S. Jin, J. Ye, *Science* **327**, 853 (2010)
7. D. Ding, J. Wu, Z. Zhou, B. Shi, X. Zou, G. Guo, *Phys. Rev. A* **87**, 853 (2013)
8. K.M. Jones, E. Tiesinga, P.D. Lett, P.S. Julienne, *Rev. Mod. Phys.* **78**, 483 (2006)
9. M. Movre, G. Pichler, *J. Phys. B* **10**, 13 (1977)
10. W.C. Stwalley, Y.H. Uang, G. Pichler, *Phys. Rev. Lett.* **41**, 17 (1978)
11. K.B. Davis, M.O. Mewes, M.R. Andrews, N.J. van Druten, D.S. Durfee, D.M. Kurn, W. Ketterle, *Phys. Rev. Lett.* **75**, 22 (1995)
12. W. Ketterle, K.B. Davis, M.A. Joffe, A. Martin, D.E. Pritchard, *Phys. Rev. Lett.* **70**, 15 (1993)
13. H.R. Thorsheim, J. Weiner, P.S. Julienne, *Phys. Rev. Lett.* **58**, 23 (1987)
14. P.L. Gould, P.D. Lett, P.S. Julienne, W.D. Phillips, H.R. Thorsheim, J. Weiner, *Phys. Rev. Lett.* **60**, 9 (1988)
15. V. Bagnato, L. Marcassa, C. Tsao, Y. Wang, J. Weiner, *Phys. Rev. Lett.* **70**, 21 (1993)
16. E. Pedrozo-Peñafiel, R.R. Paiva, F.J. Vivanco, V.S. Bagnato, K.M. Farias, *Phys. Rev. Lett.* **108**, 253004 (2012)
17. A. Amelink, K.M. Jones, P.D. Lett, P. van der Straten, H.G.M. Heideman, *Phys. Rev. A* **62**, 1 (2000)
18. P.A. Molenaar, P. van der Straten, H.G.M. Heideman, *Phys. Rev. Lett.* **77**, 8 (1996)
19. P.D. Lett, K. Helmerson, W.D. Phillips, L.P. Ratli, S.L. Rolston, M.E. Wagshul, *Phys. Rev. Lett.* **71**, 14 (1993)
20. A. Amelink, K.M. Jones, P.D. Lett, P. van der Straten, H.G.M. Heideman, *Phys. Rev. A* **61**, 4 (2000)